THE LHC FAST BCT SYSTEM: A COMPARISON OF DESIGN PARAMETERS WITH INITIAL PERFORMANCE

D. Belohrad#, L. K. Jensen, O. R. Jones, M. Ludwig, J. J. Savioz, CERN, Geneva, Switzerland

Abstract

The fast beam current transformers (FBCTs) for the Large Hadron Collider (LHC) were designed to provide bunch to bunch and turn by turn intensity measurements. The required bunch to bunch measurements together with a large machine circumference call for stringent control of the transmission bandwidth, droop and DC offsets in the front-end electronics. In addition, two measurement dynamic ranges are needed to achieve the required measurement precision, increasing the complexity of the calibration. This paper reports on the analysis of the measurement and calibration methods, discusses theoretical precision limits and system limitations and provides a comparison of the theoretical results with the real data measured during the LHC start-up.

INTRODUCTION

The FBCT measurement system (Fig. 1) is composed of the measurement device [1], front-end electronics, an acquisition system [2], and a software control system. The system was designed to comply to the measurement specification [3].

The beam current is measured using 1:40 toroid transformer from Bergoz Instrumentation. The signal is split in the RF distributor into two dynamic ranges, each of them providing measurements in two bandwidths: 200 MHz for bunch by bunch measurements and ~2 MHz for turn based measurements. The four measurement signals are independently integrated using the LHCb2002 analogue integrator ASIC, and sampled using 14 bit ADCs clocked synchronously with the beam. The entire measurement process is driven in the hardware by two Digital Acquisition Boards (DABs) [4]. Each DAB processes two integrated signals of the same bandwidth using an FPGA. The measured data are stored either in the FPGA on-chip memory, or in the external synchronous SRAM for large-volume measurements. The real-time software running in the front-end controller (FEC) provides the necessary system control, calibration procedure, conversion of the stored measurements to the number of charges, and a data publishing.

Four measurement modes are provided:

- **Capture** – a snapshot of the intensity measurement in each bunch slot for a specified number of turns
- **Turn Sum** – a total intensity measured over single LHC turn (3564 bunch measurement slot)
- **Slot Sum** – a sum of bunch slot intensities measured over specified number of turns
- **Sum Sum** – a measurement of *Turn Sum* over specified number of turns.

Each FBCT system is calibrated by 5 µs long current pulses of specific amplitudes. The calibration pulses are generated in a calibrator, implemented into a VME64x 6U board, and they are transported to the calibration circuit installed in the measurement device using 7/8” Heliflex cables.

MEASUREMENT ERROR

According to [3], the measurement error is specified in terms of absolute accuracy and resolution. Two LHC operational modes relevant to the measurement error are discussed in this article: the LHC pilot bunch injection, and the LHC ultimate SPS batch injection. The required turn-based measurement precision for both scenarios is summarised in Tab. 1.

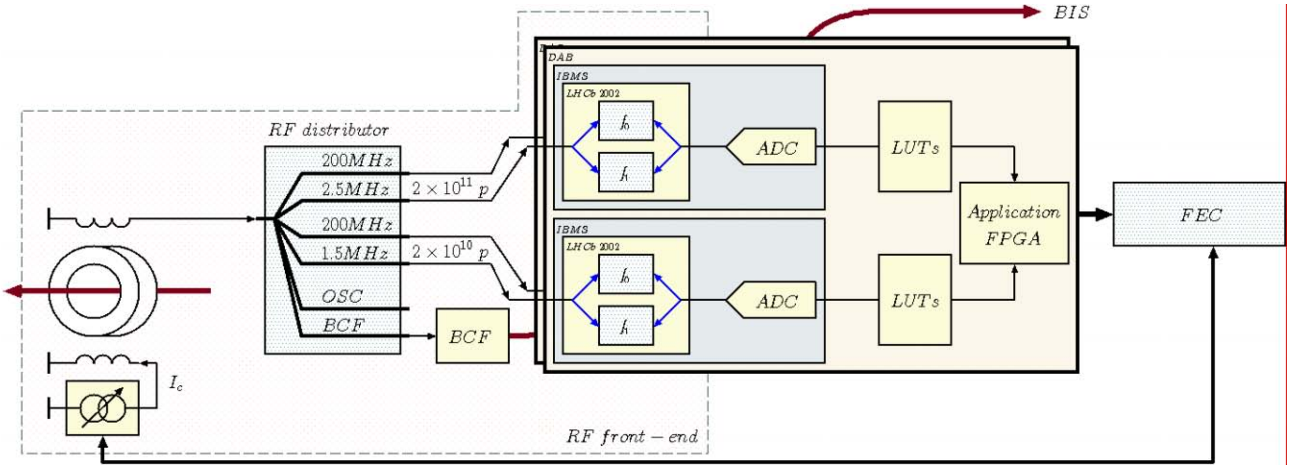

Figure 1: Block schematic of the FBCT measurement system

#david.belohrad@cern.ch

Table 1:Required measurement precision

Operational mode	**Number of charges per bunch**	**Absolute accuracy per bunch**	**Resolution**
LHC pilot	5×10^9	±20% $\pm10^9$ ch.	±20% $\pm10^9$ ch.
Ultimate SPS batch	1.7×10^{11}	±2% $\pm2\times10^9$ ch.	±1% $\pm10^9$ ch.

In order to fulfil such stringent measurement requirements the FBCT system blocks were evaluated individually, minimising the measurement error of each signal treatment stage. Following measurement error contributors were identified:

- droop of the measured beam current signal
- offsets in the front-end electronics
- calibration algorithm and accuracy of the generated calibration current
- transmission of the calibration current from the calibrator to the FBCT measurement winding

MEASUREMENT ERROR CONTRIBUTORS

Beam Current Signal Droop

The FBCT transfer function for a toroid transformer having N_s turns is defined as:

$$I_s=\frac{s\tau}{s\tau+1}\cdot\frac{I_b}{N_s}, \tag{1}$$

where $\tau=L_s/R_s$ determines the low-frequency (LF) cut-off and I_b is the beam current. L_s and R_s define the inductance and resistance of the measurement winding. The first term of Eq. (1) describes a high-pass filter. Hence the FBCT does not transfer the DC signal component and the measured signal I_s exhibits a droop. When the beam circulates in the LHC, the droop can be actively suppressed using a base-line restoration (BLR) algorithm, however the BLR is of no use at injection. This case was identified to be critical for the measurement error caused by the droop.

In order to calculate the absolute droop error for each LHC bunch slot an analytical droop model was constructed. The model uses a convolution of the transfer function Eq. (1) with a base function, defined as:

$$f(t)=\begin{cases} a[cos(b(t-kT_0))^2-1]^2 & t\in\langle kT_0;kT_0+\frac{\pi}{b}\rangle \\ 0 & t\in\langle kT_0+\frac{\pi}{b};(k+1)T_0\rangle \end{cases} \tag{2}$$

The base function describes a bunch train spaced by T_0, where each bunch is defined using constants a and b derived from the LHC longitudinal bunch size σ.

The convolved signal (Fig. 2) is used to determine the measurement error in each bunch slot of the LHC machine as a difference between the convolved signal and the original signal. The model analysis reveals, that for the case of the LHC pilot bunch, a 1% droop error is achieved using an FBCT with LF cut-off of 100 kHz.

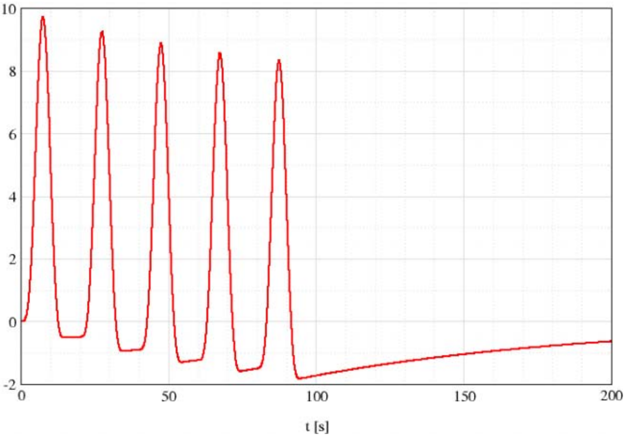

Figure 2: Result of the convolution calculation for five bunch slots and arbitrarily chosen parameters to emphasize the effect of the signal droop

Such model was applied as well to determine the required LF cut-off in case of an injection of a maximum of four SPS batches. The worst-case error exhibits at the end of the injection, and its absolute value can be determined using following generic equation:

$$E_e(k)=N_p e\cdot\frac{24\tau^5 b^4 a\left(e^{\frac{KT_0}{\tau}}-e^{\frac{KbT_0+\pi}{b\tau}}+\frac{\pi}{b\tau}-1\right)e^{-\frac{(k+1)T_0}{\tau}}}{64\mathrm{b}^4\tau^4+20\mathrm{b}^2\tau^2+1}, \tag{3}$$

where N_p is the number of charges, e is the elementary charge, K is number of injected bunches and τ is the FBCT LF cut-off. Lower-case k denotes the bunch slot number for which the error is calculated (k > K).

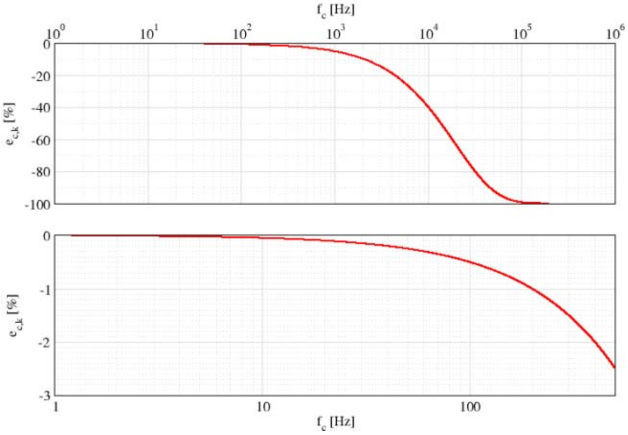

Figure 3: Relative error caused by the signal droop at the end of 4 SPS batch (288 bunches, ~8µs) injection into the LHC as a function of the FBCT LF cut-off

The result of the calculation of the relative error caused by the signal droop at the end of four-batch SPS LHC injection is shown in Fig. 3. Should the droop error be kept under 2% an FBCT having a LF cut-off lower than 400Hz is required. The toroids in the LHC have a LF cut-off approximately 200 Hz so the droop error lowers to 1%.

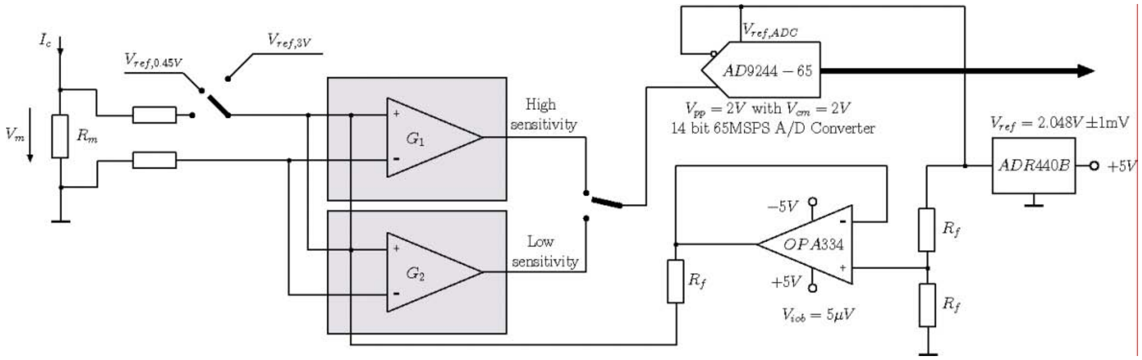

Figure 4: Acquisition system implemented into the calibrator to measure the amplitude of the current pulse sent to the calibration winding of the FBCT

Calibration algorithm

The FBCT calibration is based on a linear fit of the values measured to associated reference signals. Reference signals are provided by a calibrator generating a current pulse of a known amplitude. The pulse is sent into the FBCT calibration winding, and appropriate reference values are measured. Four measurement ranges require totally three calibration currents, as shown in Tab. 2.

Table 2:Required calibration currents

	Low bandwidth	**High bandwidth**
Low gain	650mA	650mA
High gain	12mA	40mA

Each measurement channel is calibrated using an averaged offset and a reference current measurement. 32 sample-averaging is used to reduce the noise imposed on the measured data.

The important measurement error contributor is the accuracy of the generated calibration pulse. Accuracy of the current amplitude setting is limited by the on-board amplifiers offset and gain errors as well as by the precision of the resistors. The amplifiers have high bandwidth and high slew rate, and contribute significantly to the current setting uncertainty. The actual calibrator implementation exhibits a current setting uncertainty of 1.9 mA. This is not sufficient to calibrate properly the high gain (HIGAIN) measurement channels and hence a system to measure the current sent to the calibration winding was included into the calibration pulse generator.

The current measurement is based on sampling and conversion of a voltage developed across a shunt resistor installed in the feedback of the current source amplifier (R_m). The measurement method is shown in Fig 4. The measured voltage is amplified by two fast Voltage-feedback Operational Amplifiers (VFOA). The amplifiers amplify the input signal using different gains and provide two sensitivity ranges: the high-sensitivity range performs measurements of generated currents not exceeding 150 mA in amplitude, the low-sensitivity range provides measurement of full 800 mA current span. The amplified voltage is then sampled using a 14-bit AD9244 ADC clocked synchronously with the beam.

The reference voltage for the ADC is generated by a precision 2.048±0.05% voltage source. The ADC is set up to give a reading for a positive voltage of 1 to 3 volts. The OPA334 injects into the gain blocks a DC voltage shifting the measured voltage V_m to the operational range of the ADC. It adds as well a small positive offset so that in all possible cases the ADC generates non-zero positive response when performing offset measurements.

Two references are used to calculate on-fly a linear fit of the ADC measured data to the calibration current.

Estimation of the measurement uncertainty is based on an idea of uncertainty propagation for indirect measurements of current. The type B uncertainty [5] of the measured current $I_c=V_m/R_m$ is determined using following equation:

$$u_{B,I_c}=\sqrt{\frac{u_{V_m}^2}{R_m^2}+\frac{V_m^2 u_{R_m}^2}{R_m^4}}, \qquad (4)$$

where V_m is the measured voltage, R_m the reference shunt resistor, u_{R_m} is the type B uncertainty of the resistance used and u_{V_m} is the type B uncertainty of the measured voltage.

The resistance value uncertainty is determined using widely accepted $\sqrt{3}$ rule:

$$u_{R_m}=\frac{1}{100}\cdot\frac{R_m\cdot\delta_{R_m}}{\sqrt{3}}, \qquad (5)$$

where δ_{R_m} denotes the resistance tolerance (%).

The unknown in Eq. (4) is the uncertainty of the voltage measured u_{V_m}. This value is determined from a linearisation function implemented in the calibrator's FPGA:

$$V_m=(V_{ref,1}-V_{ref,2})\cdot\frac{ADC_m-ADC_{ref,2}}{ADC_{ref,1}-ADC_{ref,2}}+V_{ref,2} \qquad (6)$$

The uncertainty propagation function Eq. (7) is applied to all the terms of Eq. (6) for both measurement ranges to determine the linearisation uncertainty u_{V_m}:

$$u_f=\sqrt{\sum_i\left(\frac{\partial f(x_0,x_1,\dots,x_i)}{\partial x_i}\cdot u_{x_i}\right)^2} \qquad (7)$$

The used reference voltages in Eq.(6) differ for each measurement range (Tab. 3), their uncertainties were determined using Eq. (7) applied on the references' transfer functions. Corresponding ADC values were measured on a real system.

Table 3:Used references for both sensitivity ranges

	High Sensitivity	**Low Sensitivity**
$V_{ref,1}$	0.45 V	3 V
$V_{ref,2}$	0 V (offset)	0.45 V

Uncertainty of the ADC measurements was determined using Eq. (8) as only integral non-linearity and resolution are major error contributors.

$$u_{ADC} = \frac{\sqrt{3}}{3} \frac{INL \cdot FSR}{2^N - 1}, \qquad (8)$$

where INL is the integral non-linearity of the ADC used and FSR is its full-scale reading.

Type A uncertainty was evaluated on the real system for both measurement ranges and all generated currents, and only the worst-case estimations of $u_{A,h}$=12.4 µA for high sensitivity, and $u_{A,l}$=84.9 µA for low sensitivity were considered (32 samples were used to estimate the uncertainty). The total uncertainty was determined using geometrical sum of both uncertainty types. Extended relative uncertainty was calculated using inclusion factor 2. The results are shown in Fig. 5. Detailed analysis can be found in [6].

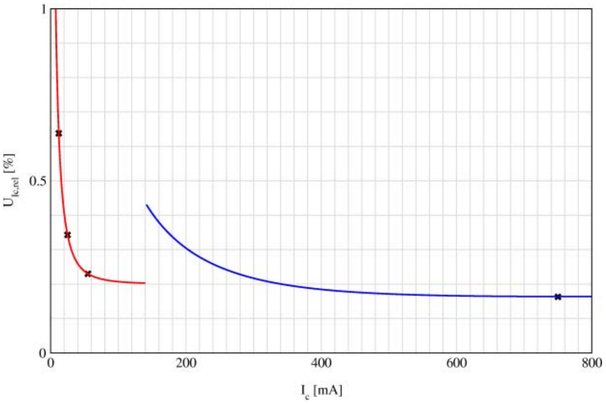

Figure 5: Relative extended uncertainty of the calibration current pulse measurement

Transmission of the calibration current from the calibrator to the measurement winding

Special attention was paid to create a well matched transmission line to transport the calibration pulse to the measurement device, and to assure a minimum signal loss due to electromagnetic coupling. Achieving this requires the calibration current generated electromagnetic field to be homogeneously distributed in the volume of the toroid. To find the best possible calibration turn winding arrangement a set of them were tested.

The schematic drawing of the winning candidate is shown in Fig. 6. The test calibration turns were fabricated using 0.381 mm thick NY9220 RF substrate. Four connection types, dividing the current to 4, 6, 8 and 16 parallel branches were tested.

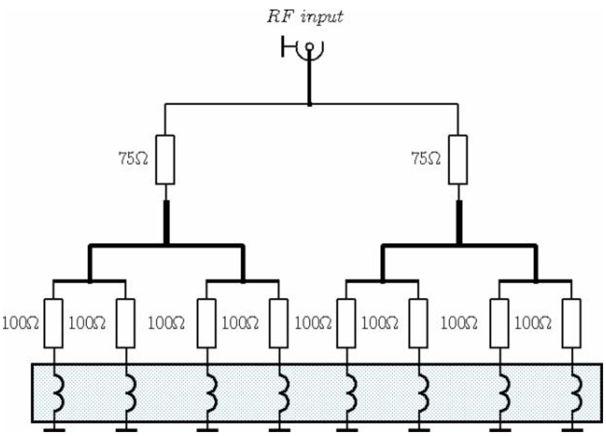

Figure 6: The LHC FBCT calibration turn

The charge transmission ratio was calculated comparing the charge measured at the FBCT output to the value calculated from the charge measured at the input of the calibration turn. Summary of the results is shown in Tab 4. Mechanical constraints did not permit to use the 16 branches, hence a compromise 8 branch version was used.

Table 4:Transmission ratio for tested calibration circuits

Number of branches	**Coefficient of transmission [%]**
4	87.2
6	95.2
8	99.3
16	99.8

Offsets in the Front-end electronics

The used analogue integrator works with input voltages of approximately 2 V and provides full-scale (FS) charge measurement of 62pC. Any DC signal present at its input represents an error signal at its output. In extreme case the DC input signal would saturate the integrator and the useful signal would be lost. Although the DC signal can be calibrated away, it lessens the dynamic range of the used integrator.

The RF distributor generates the signals for the measurement channels integrators. As each channel provides measurement using different gain and bandwidth, the provided signals may exhibit output DC offsets in range of hundreds of millivolts. This is especially case of low-bandwidth high-gain measurement channel, which must heavily amplify (+30dB) the low mean value LHC pilot beam signal. An active output offset suppression was developed to minimise the effect of the DC voltage [2]. As shown in Fig. 7, the offsets are limited to theoretical 500 µV, however much better mean offset of 47 µV was measured on a lot of 20 fabricated RF distributors. This corresponds to 0.05% of the available dynamic range.

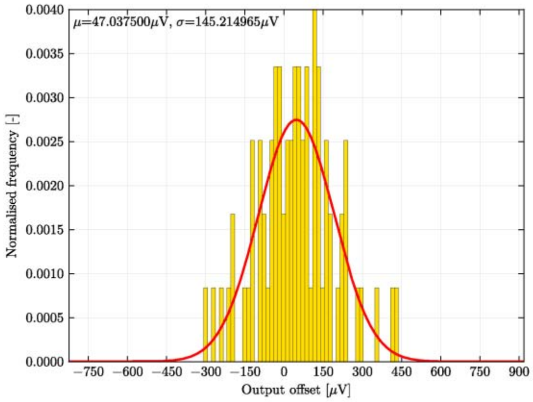

Figure 7: Normalised histogram of DC offsets measured at all outputs of RF distributor fabrication batch

MEASUREMENT RESULTS

In order to evaluate the performance of the measurement method the implemented FBCT systems were calibrated, and their measurements were compared to the independently calibrated DC current transformers (DCCTs). One such comparison is shown in Fig.8.

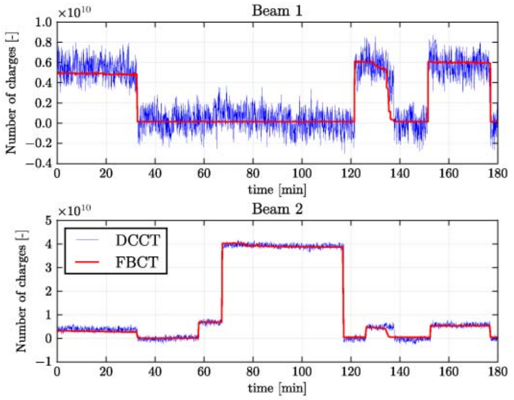

Figure 8: Comparison of independently calibrated measurements of the DCCTs and FBCTs installed in the LHC rings

The red traces correspond to the FBCTs measurements, the blue traces depict the DCCTs measurements. Top graph shows measurement of the single LHC pilot bunch, circulating in *beam 1*, bottom graph is the measurement of cumulated intensity of ≈4×10^{10} charges circulated in *beam 2*. The two independent measurement systems exhibit high degree of match. Further analysis reveals the measurement difference better than 0.5%

Table 5 summarises the noise floor measurements. As expected, the noise mean value is close to zero due to calibration and offset suppression. Its standard deviation, measured using 3564x10 samples (corresponds to ten LHC revolution periods) sets the resolution limits for future fast dI/dt measurements.

Table 5:No-beam measurements of single FBCT measurement system installed in the LHC ring

Channel	***Mean value*** **[# charges]**	***Standard deviation*** **[# charges]**	***STD relative to FS*** **[%]**
HIGAIN HIBW	-0.7×10^{6}	1.3×10^{7}	0.09
HIGAIN LOBW	0.6×10^{6}	6.2×10^{7}	0.42
LOGAIN HIBW	10.3×10^{6}	1.6×10^{8}	0.1
LOGAIN LOBW	-1.7×10^{6}	1.4×10^{8}	0.1

CONCLUSION

The FBCTs installed in the LHC were designed to satisfy the specification [3]. Although the devices were not fully tested with all possible variants of the beams, the achieved measurement accuracy on currently used LHC beams is in accordance with the specifications. This is proven as well by long-term match of the DCCT and FBCT measurements.

The noise figures measured on all measurement channels assure an optimal data source for the fast dI/dt measurement, which is currently being implemented.

The FBCT system is constantly improving as more experience is gained during the LHC operation. Its functionality was so far verified only using limited LHC injection patterns and the 'ultimate' proof of functionality will be obtained when more complex injection and acceleration scenarios are measured.

ACKNOWLEDGEMENT

The authors wish to thank to Assoc. Prof. P. Kaspar from Czech Technical University in Prague for his fruitful hints and help with the uncertainty calculus.

REFERENCES

[1] D. Belohrad, P. Odier, S. Thoulet, S. Longo: “Mechanical Design of the Intensity Measurement Devices for the LHC”, DIPAC'07, Venice, Italy, March 2007

[2] D. Belohrad, O. R. Jones, M. Ludwig, J. J. Savioz: “Implementation of the electronics chain for the Bunch by Bunch Intensity Measurement devices for the LHC”, DIPAC'09, Basel, Switzerland, May 2009

[3] C. Fischer, R. Schmidt: “On the measurements of the beam current, lifetime and decay rate in the LHC rings”, LHC-BCT-ES-0001, EDMS 359172, CERN, Geneva, Switzerland, January 2005

[4] Jones, O. R.: “VME64x Digital Acquisition Board for the LHC Trajectory and Closed orbit System”, LHC-BP-ES-0002, EDMS 410295, CERN, Geneva, Switzerland, March 2004

[5] JCGM 100:2008: “Evaluation of measurement data – Guide to the expression of uncertainty in measurement”, Joint Committee for Guides in Metrology, September 2008

[6] Belohrad, D.: “Fast Beam Intensity Measurements for the LHC”, Doctoral Thesis, to be published at Czech Technical University in Prague, 2010